Alkaline cations dramatically control molecular hydrogelation by an amino acid-derived anionic amphiphile

*César A. Angulo-Pachón, Victor Pozo and Juan F. Miravet**

Department of Inorganic and Organic Chemistry
Universitat Jaume I
12071 Castelló de la Plana, Spain
E-mail: miravet@uji.es

Keywords: molecular hydrogel, anionic surfactants, stimuli-responsive hydrogel,

ABSTRACT:

Understanding the factors that control the formation of (supra)molecular hydrogels permits a rational tuning of their properties and represents a primary challenge for developing smart biocompatible soft materials. Hydrogel formation by molecular amphiphilic anions at millimolar concentrations is counterintuitive, considering the solubility of these species in water. Here we report hydrogel formation by a simple anionic molecular amphiphile and a rationale for the fibrillisation process observed. The studied molecule, **DodValSuc,** consists of a 12C alkyl chain, an L-valine unit and a terminal succinic acid moiety. Hydrogelation depends to a large degree on the nature and concentration of the alkaline cations present in the medium (Li^+, Na^+ or K^+). As a result, gelation efficiency and properties like thermal stability or rheology are highly tunable using the alkaline cation present or its concentration as variables.

A detailed study is reported, which includes the determination of minimum gelation concentration (MGC) by tabletop rheology, critical micelle concentration (CMC) using pyrene as a fluorescent probe, thermal stability (solubility) by ^{1}H NMR, the morphology of the fibres by transmission electron microscopy (TEM), crystallinity by X-ray diffraction (XRD) and gel strength by oscillatory rheology. Additionally, dynamic light scattering (DLS) was used to evaluate the size of the micelles and permitted monitoring of the fibrillisation process.

Altogether, the results are consistent with the formation of micelles that experience head crystallisation and subsequent aggregation into crystalline fibres. The alkaline cations play a

crucial role in providing the cement that glues together the gelator molecules, making their concentration a critical parameter for gelation efficiency and properties. Furthermore, the gelation-promoting effects are inversely correlated with the size of the cations so that the highest thermal stability and rheological strength were found for the hydrogels formed in the presence of Li^+

Introduction

Molecular (supramolecular) gels are built from low molecular weight molecules which form self-assembled solvent-percolating fibrillar networks. These soft materials have been studied extensively during the last decades.[1–4] In particular, molecular hydrogels are of great interest because of their biomedical applications, such as controlled therapeutic delivery, tissue engineering or wound healing.[5–8]

A distinctive property of molecular gels is their intrinsic stimuli responsiveness associated with the non-covalent nature of the interactions that hold together the fibrillar network. Often, the gel can be reversibly assembled/disassembled in response to different stimuli such as temperature, salts, light, enzymes or different chemical species.[9–11] Also, stimuli responsiveness permits gel-to-gel transitions, affording reconfigured fibrillar networks.[12]

In particular, pH changes have often triggered molecular hydrogel assembly/disassembly. For example, different molecular gelators that experience transitions from cationic to neutral species upon increasing pH values have been reported.[13–16] Also, a pH decrease associated with the protonation of anions such as carboxylates can promote hydrogelation.[17–19] Commonly, the rationale behind pH-regulated molecular hydrogel formation is that ionic species are water soluble, precluding aggregation, while neutralisation initiates a favourable self-assembly and gelation process.

However, hydrogel formation is not at all restricted to neutral species. A well-known case corresponds to alginate macromolecular hydrogels, which form in the presence of low concentrations of divalent cations that crosslink the polysaccharide chains via complexation with the carboxylate units.[20] As for molecular gels, anionic low molecular weight species, mainly carboxylates[21,22,31–35,23–30] or sulfonates,[36,37]can also form hydrogels. Most carboxylate-type molecular hydrogelators present an amphiphilic structure, although bolaamphiphiles[24,31,32] have also been reported. In the case of carboxylate amphiphiles, n-alkyl chains are a common

motif.[24] Still, the hydrophobic moiety can also be an aromatic unit,[26,27,34] a bile acid,[23,24] or a triterpenoid.[31] The carboxylate unit can be part of an amino acid or dipeptide unit.[25,28] The molecules used in this work present an n-alkyl chain, an amino acid unit and a terminal carboxylate, which is introduced upon reacting the amino group with a dicarboxylic acid (see Scheme 1), a motif already used in some anionic hydrogelators reported previously by other groups[21,22] and us.[19]

Considering the expected electrostatic repulsion in the self-assembled fibres, the formation of molecular gels by aggregation of anionic species is counterintuitive at first glance. In this regard, several possible driving forces for the self-assembly have been proposed, such as complementary hydrophobic and hydrogen bonding interactions[21] or the increased ionic strength of the media leading to charge screening and salting-out effects.[22,29,32] The formation of tight ion pairs between carboxylates and ammonium or guanidium units has also been used to rationalise hydrogel formation.[23,24,27] In some cases, hydrogelation is triggered by adding a cationic surfactant.[21,31]

Here we report that simple anionic amphiphiles, see Scheme 1, can form hydrogels easily in aqueous media, showing a unique behaviour in terms of responsiveness to the presence of alkaline cations and temperature, affording highly tunable soft materials. Up to our knowledge, we report an unprecedented detailed study of the mechanism and responsiveness of gels formed by aggregation of anionic molecules and the role of cations based on the use of complementary information obtained from NMR spectroscopy, electron microscopy, dynamic light scattering (DLS), X-ray diffraction and rheology. Overall, the results presented aim to contribute to the rational design of smart aqueous soft materials.

Results and discussion

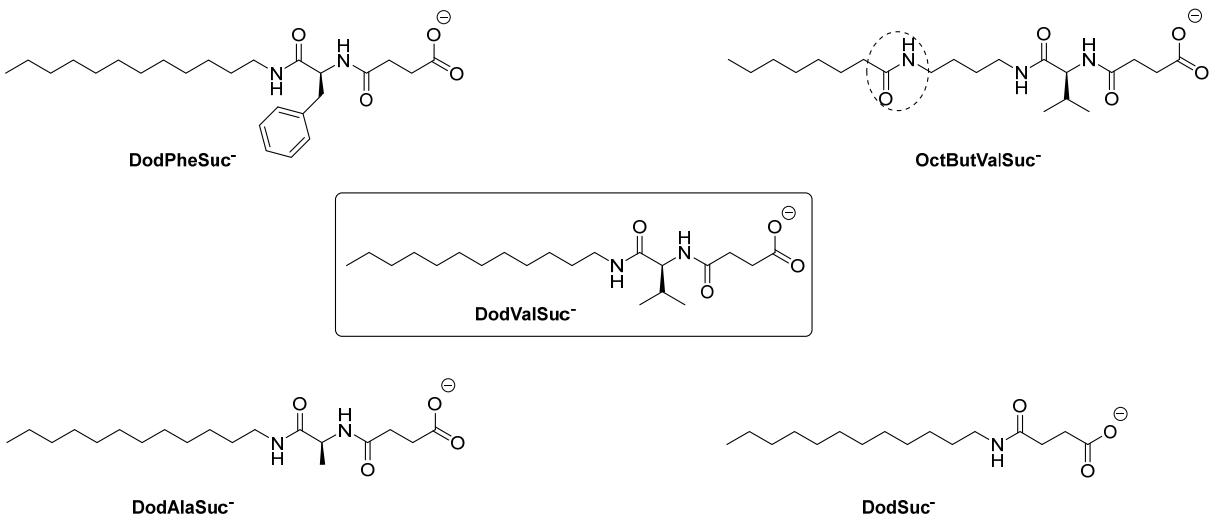

Scheme 1. Structure of the molecules studied as hydrogelators.

The main compound of this study, **DodValSuc**, contains an n-alkyl hydrophobic tail, the amino acid L-valine, and a terminal anionic carboxylic group. Two analogue compounds were prepared to replace the L-valine unit with L-phenylalanine (**DodPheSuc**) and L-alanine (**DodAlaSu**). Compounds **DodValSuc** and **DodPheSuc** were prepared previously by us for the study of the hydrogelation capabilities of their non-ionic, carboxylic acid form.[19] Additionally, here we report on analogues **DodValSuc** without the amino acid unit (**DodSuc**) and with an amide bond in the tail, increasing polarity and H-bond formation capabilities (**OctButValSuc**). In this latter case, the preparation involved monoprotection of 1,4-butanediamine and N-acylation with octanoyl chloride. For detailed synthetic procedures, see the Experimental Section.

The formation of hydrogels by the carboxylate form of **DodValSuc** was discovered serendipitously. Initially, this compound was dissolved in aqueous NaOH to form gels upon acidification and consequent formation of the non-charged carboxylic acid species.[19] Unexpectedly, in some cases, gel formation was observed for the starting solutions before acidification (pH > 11). In the first instance, gel formation by anionic **DodValSuc** showed poor reproducibility, ascribable to the strong dependence on sodium cation concentration and

temperature revealed below. These preliminary results prompted us to conduct a detailed study of the aggregation process resulting in gelation.

Minimum gelation concentration (MGC) values of **DodValSuc** in water (pH > 10) were determined in a medium with a controlled concentration of the alkaline cations Li^+, Na^+ and K^+ as well as a thermostated temperature of 25 ºC. For this purpose, **DodValSuc** was ionised and dissolved in water in the presence of a slight excess of the corresponding alkaline hydroxide. The desired concentration of alkaline cation was achieved by adding its chloride salt. The presence of a gel was assessed in the first place by tabletop rheology using the vial inversion procedure.[38]

As seen in Figure 1, gelation efficiency depends very much on the nature and concentration of the alkaline cation present in the medium. For example, the MGC values in the presence of 0.4 M K^+, Na^+ or Li^+ are 49, 10 and 7 mM, respectively. Also, for a given cation, its concentration has a striking effect on hydrogel formation. Taking the system with Na^+ as an example, the MGC values at 0.2 M and 0.6 M are 29 and 4 mM, respectively. In Figure 2, pictures of vials containing gels are shown. For a concentration of **DodValSuc** of 26 mM, an opalescent colloid is observed for $[K^+]$ = 0.4 M. Still, a self-sustained hydrogel is obtained for $[K^+]$ = 0.6 M. Also, a gel formed in the presence of 0.6 M Li^+ is depicted in Figure 2, showing a related behaviour to that of the system with K^+, but using a much lower gelator concentration.

Systems without alkaline cations were assayed employing, respectively, tetrabutylammonium (TBA) hydroxide and chloride as base and electrolyte. No gel was formed in a concentration range of 0.2-1 M of TBACl, remaining the samples as solutions.

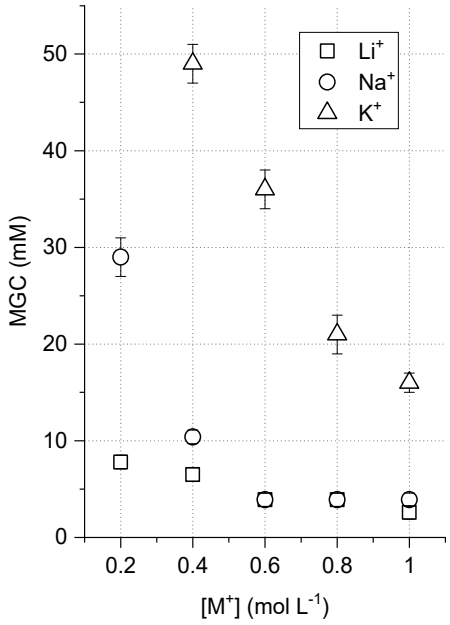

Figure 1. Minimum gelation concentration values of **DodValSuc** in water at 25 ºC in the presence of different alkaline cations (pH > 10).

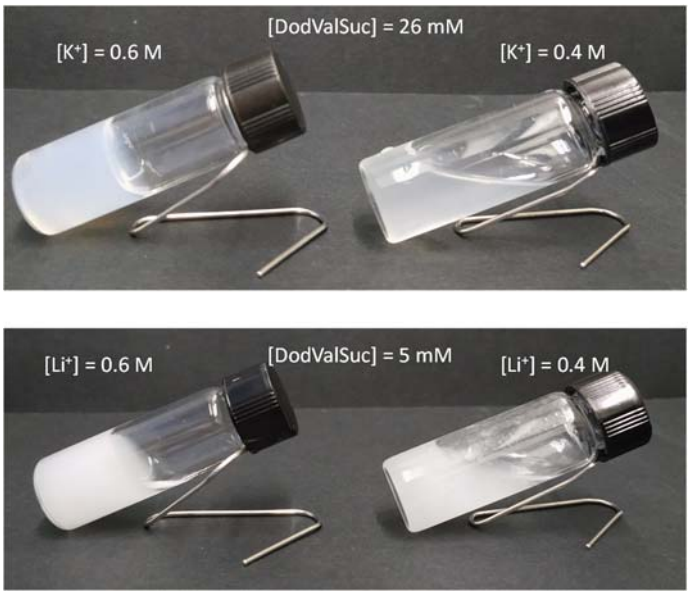

Figure 2. Pictures of gels and colloidal dispersions formed by **DodValSuc** in basic water in the presence of K^+ and Li^+ cations.

A proposed rationale for the influence of the cations on MGC values is based on the fact that deprotonated **DodValSuc** is an anionic amphiphile capable of forming conventional fluid micelles. The micelles would experience a head crystallisation process in the presence of the alkaline cations, resulting in fibrillisation and gel formation (see Scheme 2). The evolution of spherical fluid micelles upon head crystallisation into transient disks that further evolve into rods (fibrils) was reported in detail by Furhop.[39,40] Seemingly, the crystallisation effect is much stronger for the small Li^+ cation than for the bigger and polarisable K^+ species, being Na^+ cations in between.

Considering the potential use of these hydrogels in biologically related applications, the gelation properties were also assayed in a TRIS (tris(hydroxymethyl)aminomethane) buffered medium with a final pH of 7. The amount of alkaline cation was regulated by adding the corresponding chlorides. The results coincided with those obtained at basic pH values, as expected, taking into account that the molecule should be in its carboxylate form in media at neutral pH.

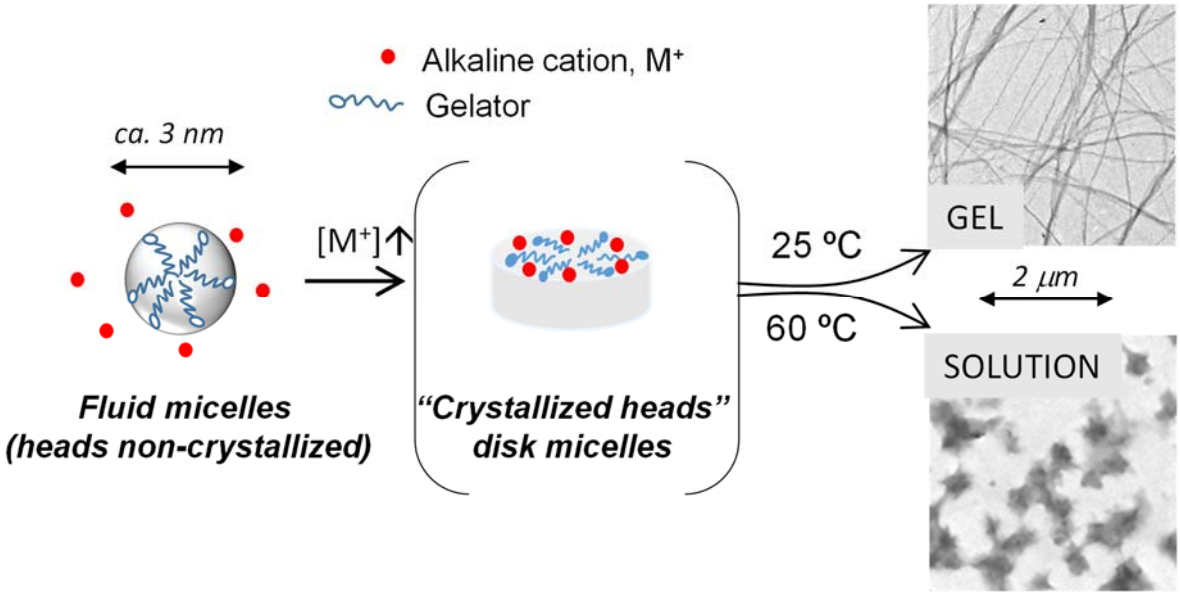

Scheme 2. Pictorial representation of the micelle crystallisation process and evolution of the transient species into gel fibres or particles.

The influence of cations on critical micelle concentration (CMC) was studied for **DodSucVal**. CMC values were determined using pyrene as a fluorescent probe. It has been shown extensively that the ratio of the first (373 nm) and third (384 nm) peaks of the emission spectrum of pyrene is susceptible to the polarity of the environment and is especially suited to detect micelle formation.[41] As seen in Figure 3, CMC values determined in this way are in the range of ca. 0.2-0.05 mM and show a dependence on the nature of the cation and its concentration. These values are one or two orders of magnitude lower than a conventional anionic surfactant like SDS (CMC = 8 mM). For Li^+, CMC decreases continuously from 0.13 mM at 0.2 M to 0.02 at 0.8M. In the case of Na^+, there is a steep decrease in CMC values upon increasing its concentration up to 0.8 M. However, for K^+, the CMC value is invariable, ca. 0.08 mM, for values above 0.4 M.

Although both CMC and MGC show dependence on the nature and concentration of the alkaline cations, there is no direct correlation between them. For example, although changing the concentration of K^+ from 0.4 M to 1 M reduces the MGC from 49 to 16 mM, the value of CMC is similar in this range of concentrations, ca. 0.08 mM. Also, 0.2 M solutions of the cations show values of CMC relatively similar (ca. 0.1-0.2 mM), but the MGC value dramatically changes with values of 8 mM and 29mM, respectively, for Li^+ and Na^+ while no gel formation at 50 mM was observed for K^+. These results support that the micelles experience a cation-promoted aggregation yielding gel fibres, strongly dependent on the alkaline cation species.

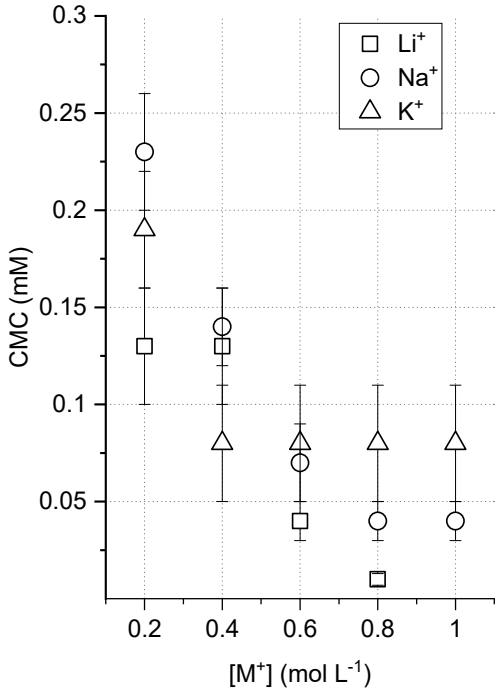

Figure 3. Critical micelle concentration values of **DodValSuc** in water at 25 ºC in the presence of different alkaline cations (pH > 10).

The thermal stability of the gels could be nicely monitored using ^{1}H NMR spectroscopy to evaluate the solubility of the gelator. Gel fibres are NMR silent, and the free gelator molecules can be detected upon gel disassembly.[42] Figure 4 collects the variation of the solubility of **DodValSuc** at pH > 10 with the temperature in water in the presence of the different concentrations of Na^{+}. It can be observed how the solubility presents a pronounced exponential dependence. Up to a specific critical temperature, the gel fibres are not temperature sensitive, but once a temperature threshold is reached, a dramatic solubility increase is observed. This critical temperature can be considered the Kraft temperature of the system.[43,44] Below this temperature, the micelles aggregate and become insoluble. As shown in Figure 4, the Kraft temperature is highly dependent on the concentration of Na^{+}, revealing its crucial role in micelle aggregation. The critical solubilisation temperatures are ca. 20ºC, 30ºC and 35ºC, respectively,

for solutions with a concentration of Na^+ of 0.2 M, 0.6 M and 1 M, pointing to clear stabilisation of the fibres by the presence of the cation.

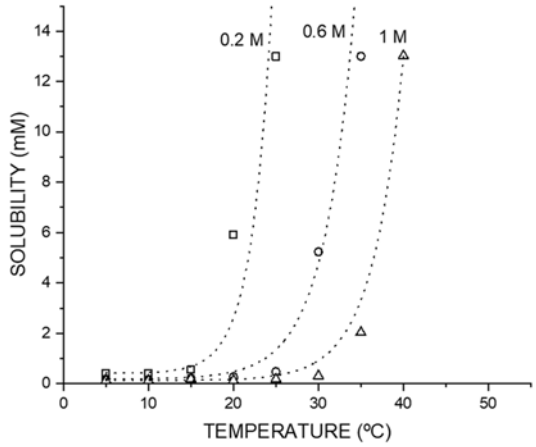

Figure 4. Variable temperature solubility study of **DodValSuc** in water at 25 ºC in the presence of different concentrations of Na^+ (pH > 10).

The nature of the cation has an even more substantial influence on the Kraft temperature, as observed in Figure 5. For a given concentration of 1 M of cation, the gels formed in the presence of Li^+ present thermal stability up to ca. 70 ºC. However, the gel formed by Na^+ dissolves at ca. 30 ºC and that of K^+ at ca. 20 ºC.

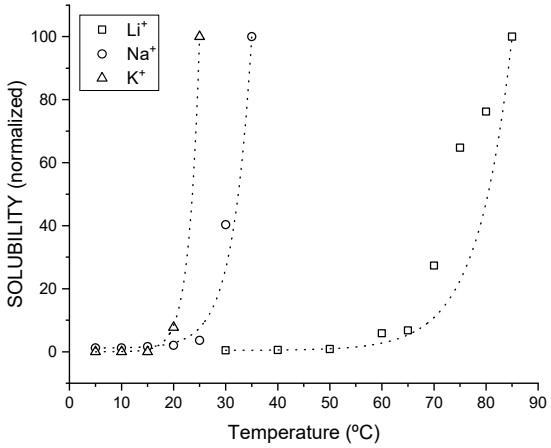

Figure 5. Variable temperature solubility study of **DodValSuc** in water at 25 ºC in the presence of 1 M Li^+, Na^+ or K^+ (pH > 10).

The fibrillar network of the hydrogels was observed by transmission electron microscopy (TEM, Figure 6, top). A typical pattern for molecular hydrogels constituted by curved fibres was observed in the presence of Na^+ and K^+, but in the case of Li+ straight fibres were predominant. This morphological change could reflect the stronger cementing ability of the Li^+ cations. TEM micrographs were also obtained by depositing a hot solution (60ºC) of a dissolved gel onto the microscopy grid. Figure 6, bottom, reveals nanoparticles of ca. 200 nm. A rationale for this observation is that nanometric particles from micelle aggregation are stable in solution at temperatures above the Kraft point. These particles would represent a polymorph of the fibres formed at lower temperatures.

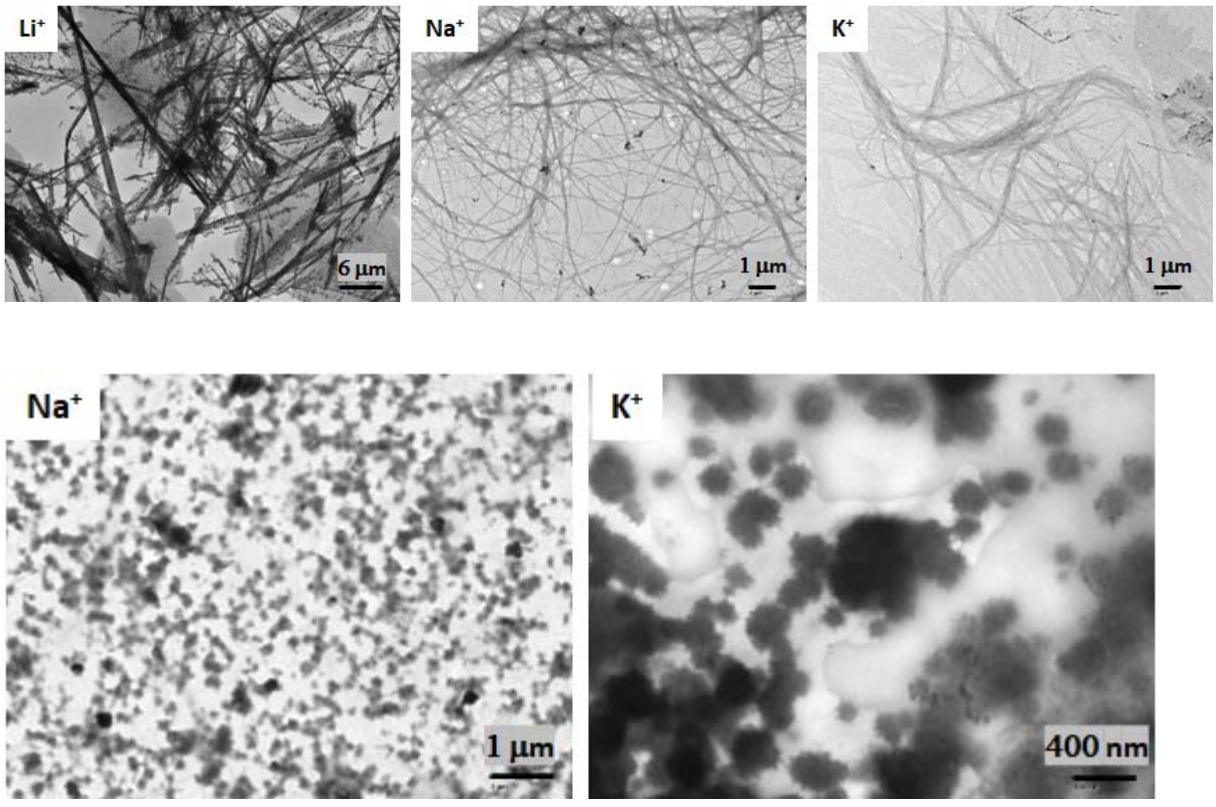

Figure 6. Top: TEM images from hydrogels of **DodValSuc** in the presence of 1 M alkaline cations. Bottom: TEM images from samples of solutions of **DodValSuc** taken at 60ºC in the presence of 1 M alkaline cations.

A dynamic light scattering (DLS) analysis of the aggregation in the presence of Na^+ cations at different concentrations and temperatures agreed with the formation of discrete nanometric particles in these systems. Figure 7, left, shows that for a solution with a low concentration of

sodium, 0.05 M, objects with an apparent diameter of ca 5 nm and 300 nm are present, corresponding to micelles and aggregated micelles. Upon increasing the concentration of Na^+ to 1 M, micelles are hardly detected. The system is composed mainly of the mentioned nanoparticles and large macroscopic aggregates associated with fibrillisation (see the peak at an apparent diameter higher than ca. 3 μm). In Figure 7, right, the effect of temperature is analysed by DLS. The fibrillated sample at 30 ºC evolves into a colloidal solution showing by DLS the disappearance of the micron-sized objects and restoring the presence of micelles in a situation resembling the sample at 30ºC with 0.05 M of Na^+.

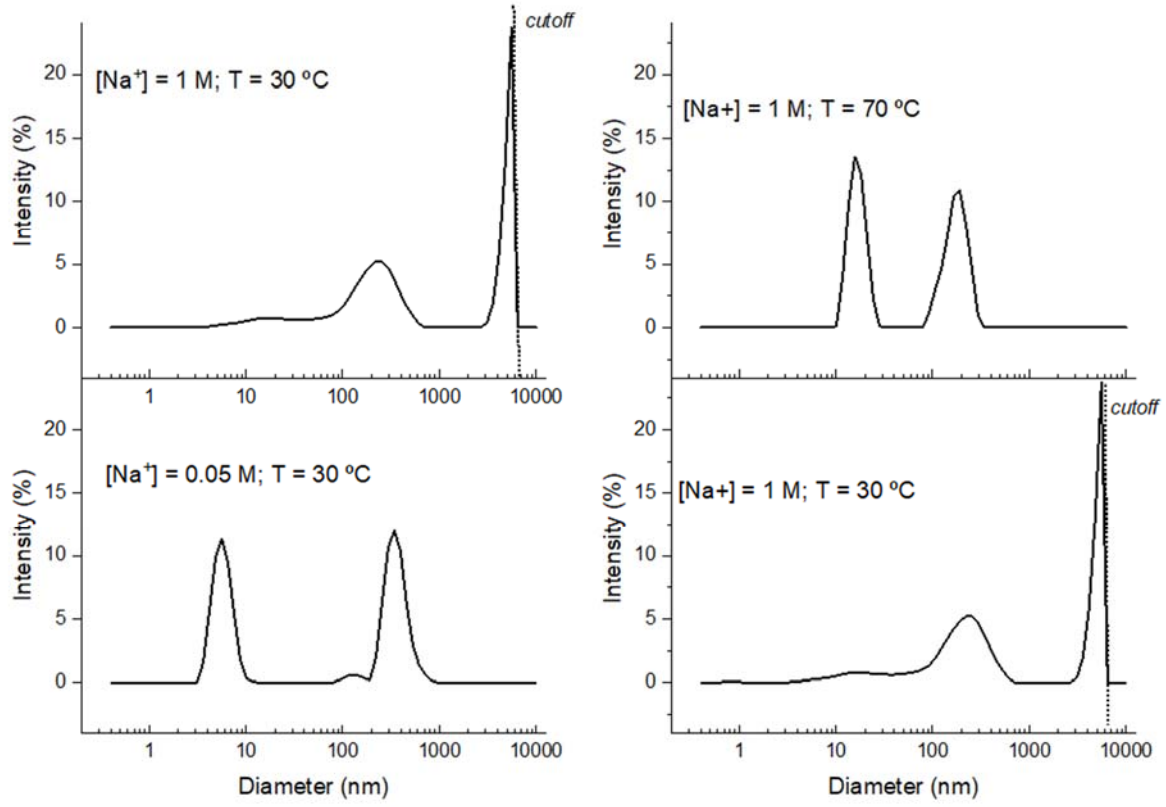

Figure 7. DLS size distribution analysis for samples with 5 mM **DodValSuc** (pH > 10).

X-Ray powder diffraction (XRD) revealed that the fibres present a crystalline packing, which supports that the cations promote a crystallisation-mediated fibrillisation. Figures 8 contains the X-ray diffraction patterns of lyophilised hydrogels formed in the presence of Li+, Na+, and

K+. All the samples show crystallinity being the longest interplanar distances observed, respectively, 38Å, 36 Å, and 37 Å. In a first estimation, this is approximately twice that of the extended length of **DodValSuc** and could be ascribed to the diameter of the micelles that originate the fibres upon aggregation. The xerogel formed in the presence of sodium shows three interplanar distances, related by 1/2, namely, 36 Å, 18Å and 9 Å. This pattern would agree with orthogonal phases (orthorhombic, tetragonal, or cubic), presenting three 90º angles in the cell unit. Alternatively, the pattern could come from a hexagonal phase with three 120º angles in the cell unit. More diffraction peaks would be required to ascertain the crystalline system.

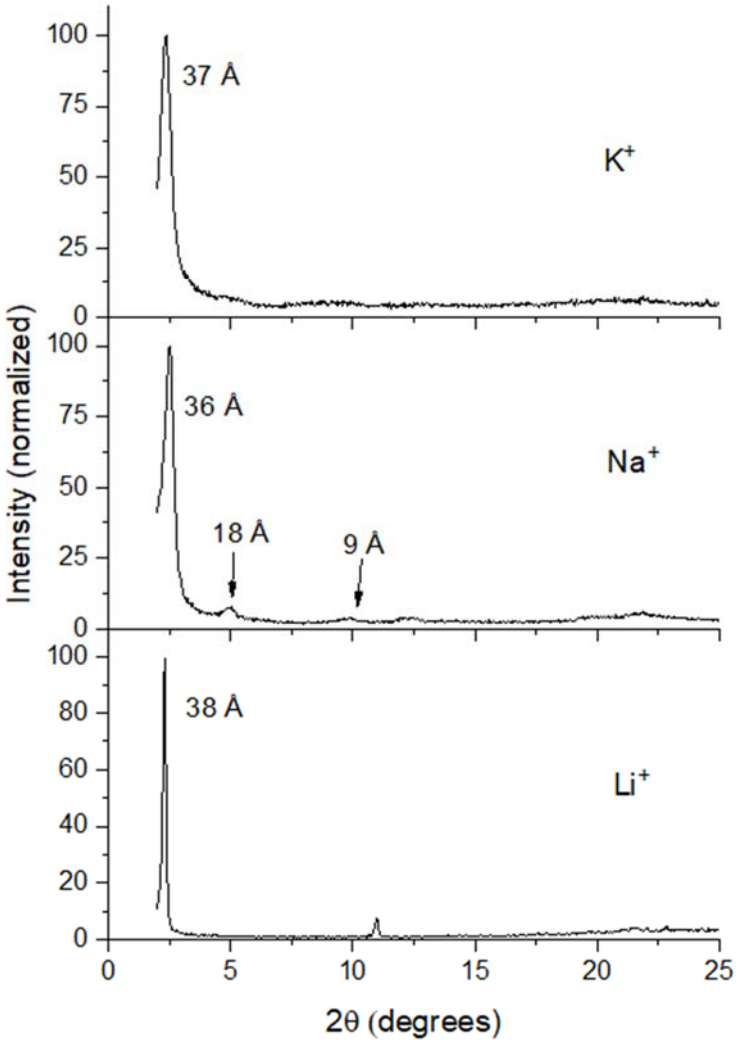

Figure 8. XRD analysis of xerogels obtained from hydrogels of **DodValSuc** by lyophilisation.

Mechanical strength is commonly a property of paramount relevance in hydrogels. Therefore, a study was carried out to assess how the alkaline cations affect the rheological properties of the gels formed by **DodValSuc**. Oscillatory stress sweeps were carried out for gels formed in the presence of the different cations (1 M) using the same amount of gelator. The data were acquired at a frequency range corresponding to a linear viscoelastic regime. In all the cases, the value of G' (elastic modulus) was higher than G'' (viscous modulus), a definitory characteristic of gels in terms of rheology (see Figure S2). By means of simplicity, only the G' values are shown in Figure 8. It can be seen that gel strength, considering the value of G', is highly dependent on the nature of the cation. The G' value for hydrogels formed in the presence of Li+ is ca. 12 105 Pa, while those of Na^+ and K^+ containing samples are orders of magnitude below, with values respectively of ca. 4 10^3 Pa and 8 10^2 Pa. Therefore, the effect of the cations correlates with that observed for the previous results shown above regarding MGC values and thermal stability. In this regard, it has to be considered that the higher efficiency of gelation of **DodValSuc** in the presence of Li^+ comes from a higher degree of aggregation of molecules into fibres, resulting in an increased content of fibrillated material and, consequently, stronger gels.

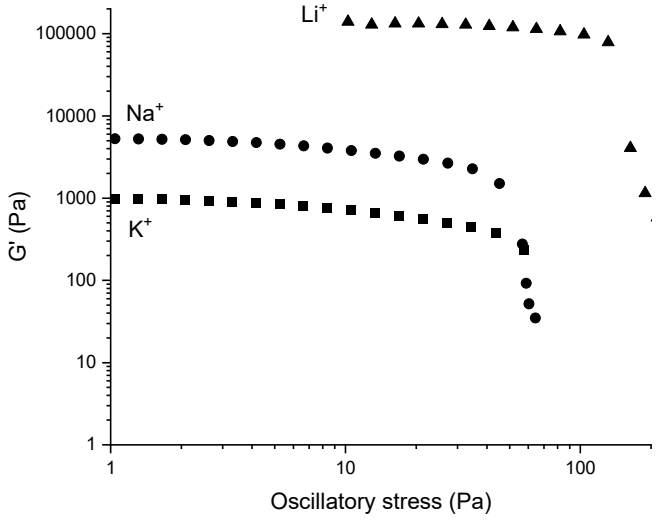

Figure 9. Rheological study of the hydrogels by oscillatory stress sweep. [**DodValSuc**] = 26 mM.

Additionally, studies of MGC and CMC were carried out for the derivatives shown in Scheme 1, aiming to evaluate how sensitive gelation properties are to structural changes. The results are collected in Table 1. Two derivatives were built by replacing the L-valine unit of **DodValSuc** with L-phenylalanine (**DodPheSuc**) and L-alanine (**DodAlaSuc**). In this way, the hydrophobic nature of the compound is modified, as shown by the ClogP values in Table 1. **DodPheSuc**, **DodValSuc** and **DodAlaSuc** have ClogP values of 3.0, 2.5 and 1.6, respectively. Notably, the higher hydrophobic nature of **DodPheVal** results in the lowest CMC value, but hydrogel formation was not observed. Instead, **DodPheSuc** formed macroscopic, phase-separated aggregates, but no gelation was achieved, indicating a 3-D aggregation rather than the anisotropic growth in one preferred direction that affords fibrillisation.[45] On the other hand, **DodAlaSuc** was too water soluble to provide efficient aggregation in water. The compound **SucDod** constitutes a simple model without the presence of the amino acid unit. Again, this compound was too soluble, and no aggregation was detected in the studied conditions. Finally, **OctButValSuc** is an analogue of **DodValSuc** with an amide unit inserted in the aliphatic tail, which presents additional hydrogen bonding sites at the cost of a considerable increment in the hydrophilic nature, affording a negative ClogP value. Remarkably this compound preserves the hydrogelation capabilities but at a much higher concentration of 85 mM.

Table 1. Critical micelle concentration (CMC) and hydrogel formation capability for various analogues of **SucValDod** in 1M aqueous NaCl. Values in parentheses indicate the estimated error.

Compound	ClogP	CMC / mM	MGC / mM
DodPheSuc	3.0	0.016 (0.003)	no gel (precipitate)
DodValSuc	2.5	0.04 (0.01)	3.9 (0.7)
DodAlaSuc	1.6	0.08 (0.03)	no gel (solution)
SucDod	1.9	0.18 (0.04)	no gel (solution)
OctButValSuc	-0.8	1.8 (0.6)	85 (12)

Conclusions

Molecular hydrogels are formed by the carboxylate form of the compound **DodValSuc,** driven by the presence of alkaline cations Li^+, Na^+ or K^+. Therefore, the nature of the cation has paramount importance in the gelation process and properties of the gel. The evidence above agrees with a gelation mechanism consisting of cation-promoted micelle head crystallisation above a critical alkaline cation concentration and subsequent aggregation into fibrils. Furthermore, the results indicate that alkaline cations act as the cement that holds together the fibres.

MGC determination by vial inversion, thermal stability by NMR and rheology reveal that the gelation-promoting capabilities of the cations follow the order $Li^+ > Na^+ > K^+$ indicating that the small diameter and poor polarizability of the Li^+ are favourable factors for the micelle crystallisation and fibre formation. Additionally, the crystalline nature of the fibres revealed by XRD diffraction supports crystallisation-driven fibrillisation.

Importantly, insight into the gelation process has been obtained by DLS, showing how the interconversion of micelles into fibres is regulated by the temperature of the medium and concentration of the cation. Also, DLS and TEM revealed the presence of ca. 200 nm diameter nanoparticles that seem to constitute a polymorph of the fibres, which is metastable at room temperature but predominates at temperatures above the gel-sol transition temperature.

Although the formation of hydrogels from anionic molecular species has been reported in quite some cases, as cited in the introduction, such dramatic effect in hydrogelation of the cation concentration and nature has not been reported so far. For example, gel formation efficiency by the carboxylate form of an L-lysine derivative was similar in the presence of Li^+ or K^+.[23] In related cases, the properties of two-component hydrogels by variation of the alkylammonium species were reported.[31,35]

In the system studied here, the alkaline cations have a strong influence not only on gelation efficiency but also on hydrogel properties. MGC values vary from 49 mM to 3mM. Gel-sol transition temperatures can be regulated within a broad temperature range from ca. 70 ºC to 20 ºC. Additionally, the cations can control the rheological elastic module with variations up to three orders of magnitude. Such versatile modulation of hydrogel properties by alkaline cations is unprecedented to our knowledge.

The tailorability of these soft materials opens the way for their use in various applications requiring stimuli-responsive hydrogels, such as drug delivery,[46] scaffolds for tissue engineering[47] or 3D printing.[48]

Experimental section

Gel preparation and determination of MGC. A stock dissolution of MOH 0.1 M (M= Li, Na or K) was prepared. Then, the corresponding amount of solid MCl was added to achieve the targeted concentration of cation (M+).

In a typical experiment, 4mg of **DodValSuc** and 1 mL of stock dissolution were introduced into a cylindrical screw-capped glass vial (8 mL, diameter =1.5 cm). The system was gently heated with a heat gun (air temperature 100 ºC) until the solid was dissolved. Then the sample was cooled by immersion into a thermostated water bath at 25ºC for 30 minutes. Finally, gel formation was checked with the inverted vial test. All determinations were done in triplicate.

Critical micelle Concentration. Samples were prepared similarly to the procedure described for MGC using water containing pyrene 1 mM. The fluorescence of pyrene was measured at different concentrations of **DodValSuc** (λ_{exc}= 334 nm). The plot of the intensity ratio of the bands at 373 nm (I_I) and 384 nm (I_{III}) vs the concentration affords a critical point ascribed to CMC.

^{1}H NMR study of solubility. Gel samples were prepared in conventional NMR tubes using the procedure described above. Samples were stabilised for 5 minutes at the desired temperature,

and signals of the gelator were integrated using as a reference an electronic signal (ERETIC procedure).

Transmision electron microscopy. TEM images were obtained using a JEOL 2100 electron microscope with thermionic gun LaB6 100 kV equipped with a GatanOrius high-resolution CCD camera. TEM samples were prepared over carbon formvar copper grids.

Dynamic light scattering. DLS measurements were carried out with a Zetasizer Nano ZS device (Malvern). Analyses were carried out using a He–Ne laser (633 nm) at a fixed scattering angle of 173°. Automatic optimisation of beam focusing and attenuation was applied for each sample. Samples were measured in 3 mL disposable poly(methyl methacrylate) cuvettes (10 mm optical path length). The particle size was reported as the average of three measurements.

X-ray powder diffraction. Data were collected at room temperature with a Bruker D4 Endeavor X-ray powder diffractometer by using Cu-α radiation. A sample of the respective freeze-dried powder was placed on a sample holder, and data were collected for 2θ

values between 2 and 40° with a step size of 0.03° and a time step of 10 s.

Rheology. A parallel plate geometry with a diameter of 25 mm was used. Oscillatory stress sweeps were carried by triplicate at 1 Hz or 10 Hz within the linear viscoelastic regime.

Synthesis. The synthesis and characterisation of **DodValSuc**, **DodPheSuc**[19] and **DodSuc**[49] were reported previously.

DodAlaSuc *((S)-4-((1-(dodecylamino)-1-oxopropan-2-yl)amino)-4-oxobutanoic acid*) was prepared similarly as **DodValSuc** and **DodPheSuc** starting from the corresponding L-alanine derivative.

^{1}H NMR (300 MHz, DMSO-d_6): δ 0.86 (t, 3H), 1.17 (d, 3H), 1.25 (br, 18H), 1.37 (t, 2H), 2.39 (m, 4H), 3.02 (m, 2H), 4.19 (quint, 1H); 7.70 (t, 1H); 8.02 (d, 1H); 12.11 (br, 1H)

^{13}C NMR (75 MHz, DMSO-d_6): δ 14.4, 18.8, 22.6, 26.7, 29.3 (br, 3C) , 29.4 (br, 4C), 29.5, 30.4, 31.2, 38.9, 48.7, 171.2, 172.4, 174.4

OctButValSuc was prepared according to Scheme 3.

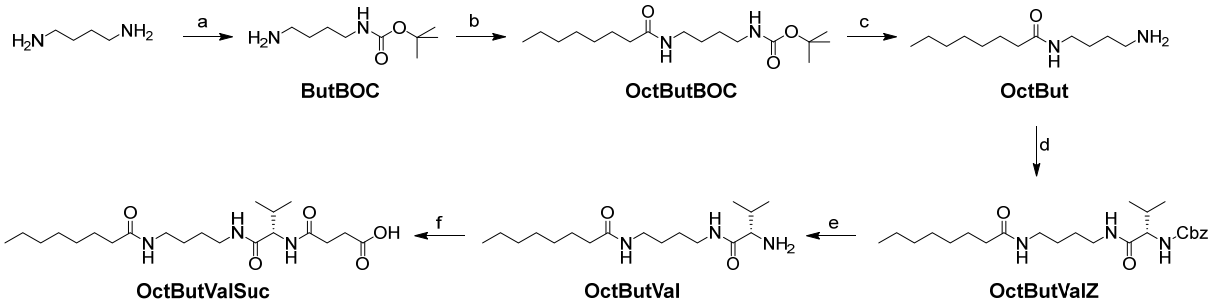

Scheme 3. Reagents and contitions for the synthesis of **OctButValSuc**: a) Boc_2O, HCl, MeOH, 2 h., 56 %; b) Octanoyl chloride, Et_3N, CH_2Cl_2, 1 h., 98%; c) TFA, CH_2Cl_2, 6 h., 99%; d) ZValOSu, THF, 16 h., 77 %; e) Pd/C, H_2, MeOH, 4 h., 100 %; f) Succinic anhydride, K_2CO_3, THF, 16 h., 37%.

ButBOC *(tert-butyl (4-aminobutyl)carbamate)* A solution of 1,4-diaminobutane (34 mmol, 1eq.) in MeOH (50 mL) previously acidified with conc. aq.HCl (34 mmol, 1 eq.) was stirred for 20 minutes at 0 ºC. Next, distilled water, 7 mL, was added, and the solution was stirred for 30 minutes more. Di-tert-butyl dicarbonate (Boc_2O) (51 mmol, 1,5 eq.) in MeOH (30 mL) was added with a dropping funnel to the previous mixture and stirred for 1 h. Then, the mixture was cooled at room temperature, and the solvent was removed under reduced pressure. The residue was suspended in 40 mL of 1 M NaH_2PO_4 sonicated for 10 minutes and the solid was filtered out. The solution was washed with diethyl ether (3x40 mL). Next, a 1 M NaOH solution was added to the aqueous phase until pH 10 and the product was extracted with AcOEt (3x 40 mL). The organic phase was dried with Na_2SO_4 anhydride and concentred under reduced pressure. The product was dried under reduced pressure and 50 ºC overnight. A white solid was obtained (56% yield).

^{1}H NMR (300 MHz, $CDCl_3$): δ 4.63 (s, 1H), 2.86 (d, J = 6.0 Hz, 2H), 2.45 (t, J = 6.7 Hz, 2H), 1.32 (bs, 2H), 1.28 – 1.20 (m, 4H), 1.18 (s, 9H).

^{13}C NMR (75 MHz, $CDCl_3$): δ 156.0 (C=O), 78.9 (C), 41.7 (CH_2), 40.3 (CH_2), 30.7 (CH_2), 28.4 (CH_3 x3), 27.4 (CH_2).

OctButBoc *(tert-butyl (4-octanamidobutyl)carbamate).* A solution of tert-butyl (4-aminobutyl)carbamate (19 mmol, 1 eq.) and triethylamine (22.8 mmol, 1.2 eq.) in dichloromethane (100 mL) was stirred at 0 ºC for 30 minutes. Then a solution of octanoyl chloride (19 mmol, 1eq.) in dichloromethane (5 mL) was added with a dropping funnel and stirred 1 h at room temperature. The mixture was washed with aq. 1 M NaH_2PO_4 (3 x 40 mL). The organic phase was dried with anhydrous $MgSO_4$, and the solvent was removed under reduced pressure. The product was dried under reduced pressure and 50 ºC overnight. A white solid was obtained (98% yield)

^{1}H NMR (300 MHz, $CDCl_3$): δ 5.81 (s, 1H), 4.67 (s, 1H), 3.26 (q, *J* = 6.1, 2H), 3.12 (q, *J* = 6.1 Hz, 2H), 2.15 (t, *J* = 7.6, 2H), 1.68 – 1.56 (m, *J* = 14.1, 6.8 Hz, 2H), 1.55 – 1.46 (m, 4H), 1.43 (s, 9H), 1.32 – 1.21 (m, 8H), 0.86 (t, *J* = 6.8 Hz, 3H).

^{13}C NMR (75 MHz, $CDCl_3$): δ 173.4 (C=O), 156.3 (C=O), 79.3 (C), 40.2 (CH_2), 39.1 (CH_2), 36.9 (CH_2), 31.8 (CH_2), 29.4 (CH_2), 29.1 (CH_2), 28.5 (CH_3 x3), 27.7 (CH_2), 26.8 (CH_2), 25.92

OctBut *(N-(4-aminobutyl)octanamide).* Trifluoroacetic acid (30 mL, 0.39 mol, 21 eq.) was added with a dropping funnel to a solution of tert-butyl (4-octanamidobutyl)carbamate (18.7 mmol, 1 eq.) in dichloromethane (50 mL) and stirred for 6 h at room temperature. Then, the solvent was removed under reduced pressure. The yellow oil was diluted with water, and a 1 M NaOH solution was added until pH 10. The product was extracted with dichloromethane (3 x 40 mL). The organic phase was dried with anhydrous Na_2SO_4, and the solvent was removed under reduced pressure. The compound was dried under reduced pressure and 50 ºC overnight. A white solid was obtained (98% yield).

^{1}H NMR (300 MHz, $CDCl_3$): δ 6.20 (s, 1H), 3.19 (q, J = 6.4 Hz, 2H), 2.68 (t, J = 6.5 Hz, 2H), 2.11 (t, J = 7.6 Hz, 2H), 1.67 – 1.35 (m, 8H), 1.33 – 1.15 (m, 8H), 0.84 (t, 3H).

^{13}C NMR (75 MHz, $CDCl_3$): δ 173.3 (C=O), 41.7 (CH_2), 39.3(CH_2), 36.9 (CH_2), 31.7 (CH_2), 30.9 (CH_2), 29.3 (CH_2), 29.1 (CH_2), 27.1 (CH_2), 25.9 (CH_2), 22.6 (CH_2), 14.1 (CH_3).

OctButValZ *(benzyl (S)-(3-methyl-1-((4-octanamidobutyl)amino)-1-oxobutan-2-yl)carbamate).* A solution of activated ester ZValOSu (2,5-dioxopyrrolidin-1-yl ((benzyloxy)carbonyl)-L-valinate) (18.3 mmol) in DME (100 mL) was added dropwise under N_2 at room temperature with a dropping funnel to a solution of **OctBut** (18.3 mmol, 1 eq.) in DME (120 mL). The mixture was stirred under N_2 for 5 h at 55 ºC. After that, the mixture was cooled to room temperature, and the solvent was removed under reduced pressure. Then the residue was poured into dissolution 0.1 M aq. HCl, then the mix was sonicated for 5 minutes. Next, it was filtered under a vacuum, and the residue was washed with water until pH = 7. The compound was dried under reduced pressure and 50 ºC overnight. A white solid was obtained (77% yield).

^{1}H NMR (300 MHz, $CDCl_3$): δ 7.43 – 7.29 (m, 5H), 6.33 (s, 1H), 5.73 (s, 1H), 5.43 (s, 1H), 5.11 (s, 2H), 3.96 (dd, *J* = 8.6, 6.3 Hz, 1H), 3.34 – 3.15 (m, *J* = 16.6, 5.6 Hz, 4H), 2.15 (t, *J* = 15.9, 8.1 Hz, 3H), 1.66 – 1.57 (m, 2H), 1.51 (s, 4H), 1.37 – 1.19 (m, 8H), 0.97 (d, *J* = 6.8 Hz, 3H), 0.92 (d, *J* = 6.8 Hz, 3H), 0.88 (t, *J* = 6.7 Hz, 3H).

^{13}C NMR (75 MHz, $CDCl_3$): δ 173.7 (C=O), 171.7 (C=O), 156.6 (C=O), 136.4 (C), 128.6 (CH x2), 128.3 (CH), 128.1 (CH x2), 67.0 (CH_2), 60.7 (CH), 39.1 (CH_2), 39.0 (CH_2), 36.8 (CH_2), 31.8 (CH_2), 31.2(CH), 29.4 (CH_2), 29.1 (CH_2), 27.0 (CH_2), 26.7 (CH_2), 25.9 (CH_2), 22.7 (CH_2), 19.4 (CH_3), 18.0 (CH_3), 14.1 (CH_3).

OctButVal *((S)-N-(4-(2-amino-3-methylbutanamido)butyl)octanamide).* Palladium on C catalyst (20% w/w) was suspended in MeOH (100 mL) and stirred under H_2 at room temperature for 10 min. Subsequently, a solution **OctButValZ** (14.1 mmol) in MeOH (50 mL) was added via a syringe, followed by stirring under H_2 at room temperature for 4 h. The reaction mixture was then filtered through Celite, and the solvent was removed under reduced pressure to yield a white solid, which was used without further purification for the next step (98 % yield).

^{1}H NMR (300 MHz, $CDCl_3$): δ 7.43 (s, 1H), 5.83 (s, 1H), 3.37 – 3.23 (m, 4H), 3.23 (d, *J* = 3.7 Hz, 1H), 2.40 – 2.23 (m, *J* = 17.7, 8.8, 5.0 Hz, 1H), 2.15 (t, *J* = 7.6 Hz, 2H), 1.69 – 1.59 (m, 2H), 1.58 – 1.47 (m, 4H), 1.38 – 1.16 (m, 8H), 0.99 (d, *J* = 7.0 Hz, 3H), 0.88 (t, *J* = 9.2, 4.3 Hz, 3H), 0.83 (d, *J* = 7.1 Hz, 3H).

OctButValSuc *((S)-4-((3-methyl-1-((4-octanamidobutyl)amino)-1-oxobutan-2-yl)amino)-4-oxobutanoic acid).* A solution of **OctButVal** (14.1 mmol, 1 eq.) in THF (150 mL) was treated at 0 ºC under N_2 with solid K_2CO_3 (53.6 mmol, 3.8 eq.). The mixture was stirred for 15 minutes at 0 ºC, after a solution of commercially available succinic anhydride (28.2 mmol, 2.0 eq.) in THF (100 mL) was added with a dropping funnel. The mixture was further stirred vigorously for 16 h at room temperature. After this time, the solution was concentrated under reduced pressure, and the crude residue was dissolved in water (100 mL). Concentrated aqueous HCl was added dropwise at 0 ºC to form a white precipitate, with final pH of ca. 2. The white solid obtained was filtered under vacuum, and the residue was washed with water (300 mL). The compound was dried under reduced pressure at 50 ºC overnight. A white solid was obtained (37% yield).

^{1}H NMR (400 MHz, D_2O): δ 3.97 (d, *J* = 7.1 Hz, 1H), 3.24 – 3.01 (m, 4H), 2.55 – 2.32 (m, 4H), 2.12 (t, *J* = 7.4 Hz, 2H), 2.04 – 1.91 (m, 1H), 1.57 – 1.37 (m, 6H), 1.27 – 1.08 (m, 8H), 0.86 (dd, *J* = 6.6, 4.8 Hz, 6H), 0.76 (t, *J* = 6.7 Hz, 3H).

^{13}C NMR (101 MHz, D_2O): δ 180.9 (C=O), 175.9 (C=O), 175.7 (C=O), 173.1 (C=O), 59.7 (CH), 38.8 (CH_2), 35.9 (CH_2), 33.0 (CH_2), 32.1 (CH_2), 31.4 (CH), 30.0 (CH_2), 28.7 (CH_2), 28.6 (CH_2), 26.2 (CH_2), 26.0 (CH_2), 25.7 (CH_2), 22.2 (CH_2), 18.6 (CH_3), 17.8 (CH_3), 13.6 (CH_3).

Acknowledgements

The authors acknowledge the financial support from the Spanish Ministry of Science and Innovation, co-funded by the European Regional Development Fund of the European Union (grants RTI2018-096748-B-I00) and Universitat Jaume I (grant UJI-B2018-30).

References

(1) Weiss, R. G. The Past, Present, and Future of Molecular Gels. What Is the Status of the Field, and Where Is It Going? *Journal of the American Chemical Society*. 2014, pp 7519–7530. https://doi.org/10.1021/ja503363v.

(2) Draper, E. R.; Adams, D. J. Low-Molecular-Weight Gels: The State of the Art. *Chem*. 2017, pp 390–410. https://doi.org/10.1016/j.chempr.2017.07.012.

(3) Amabilino, D. B.; Smith, D. K.; Steed, J. W. Supramolecular Materials. *Chemical Society Reviews*. 2017, pp 2404–2420. https://doi.org/10.1039/c7cs00163k.

(4) Steed, J. W. Supramolecular Gel Chemistry: Developments over the Last Decade. *Chem. Commun.* **2011**, *47* (5), 1379–1383. https://doi.org/10.1039/c0cc03293j.

(5) Hirst, A. R.; Escuder, B.; Miravet, J. F.; Smith, D. K. High-Tech Applications of Self-Assembling Supramolecular Nanostructured Gel-Phase Materials: From Regenerative Medicine to Electronic Devices. *Angew. Chemie - Int. Ed.* **2008**, *47* (42), 8002–8018. https://doi.org/10.1002/anie.200800022.

(6) Du, X.; Zhou, J.; Shi, J.; Xu, B. Supramolecular Hydrogelators and Hydrogels: From Soft Matter to Molecular Biomaterials. *Chemical Reviews*. American Chemical Society 2015, pp 13165–13307. https://doi.org/10.1021/acs.chemrev.5b00299.

(7) Falcone, N.; Kraatz, H. B. Supramolecular Assembly of Peptide and Metallopeptide Gelators and Their Stimuli-Responsive Properties in Biomedical Applications. *Chemistry - A European Journal*. John Wiley & Sons, Ltd September 25, 2018, pp 14316–14328. https://doi.org/10.1002/chem.201801247.

(8) Webber, M. J.; Dankers, P. Y. W. Supramolecular Hydrogels for Biomedical

Applications. *Macromolecular Bioscience*. Wiley-VCH Verlag January 1, 2019. https://doi.org/10.1002/mabi.201970001.

(9) Jones, C. D.; Steed, J. W. Gels with Sense: Supramolecular Materials That Respond to Heat, Light and Sound. *Chem. Soc. Rev.* **2016**, *45* (23), 6546–6596. https://doi.org/10.1039/c6cs00435k.

(10) Dolores Segarra-Maset, M.; Nebot, V. J.; Miravet, J. F.; Escuder, B. Control of Molecular Gelation by Chemical Stimuli. *Chem. Soc. Rev.* **2013**, *42* (17), 7086–7098. https://doi.org/10.1039/c2cs35436e.

(11) Sun, Z.; Huang, Q.; He, T.; Li, Z.; Zhang, Y.; Yi, L. Multistimuli-Responsive Supramolecular Gels: Design Rationale, Recent Advances, and Perspectives. *ChemPhysChem*. 2014, pp 2421–2430. https://doi.org/10.1002/cphc.201402187.

(12) Panja, S.; Adams, D. J. Stimuli Responsive Dynamic Transformations in Supramolecular Gels. *Chem. Soc. Rev.* **2021**, *50* (8), 5165–5200. https://doi.org/10.1039/D0CS01166E.

(13) Lange, S. C.; Unsleber, J.; Drücker, P.; Galla, H. J.; Waller, M. P.; Ravoo, B. J. PH Response and Molecular Recognition in a Low Molecular Weight Peptide Hydrogel. *Org. Biomol. Chem.* **2015**, *13* (2), 561–569. https://doi.org/10.1039/c4ob02069c.

(14) Okafor, I. S.; Wang, G. Synthesis and Gelation Property of a Series of Disaccharide Triazole Derivatives. *Carbohydr. Res.* **2017**, *451*, 81–94. https://doi.org/10.1016/j.carres.2017.09.008.

(15) Wang, W. Z.; Gao, C.; Zhang, Q.; Ye, X. H.; Qu, D. H. Supramolecular Helical Nanofibers Formed by Achiral Monomers and Their Reversible Sol–Gel Transition. *Chem. - An Asian J.* **2017**, *12* (4), 410–414. https://doi.org/10.1002/asia.201601733.

(16) Externbrink, M.; Riebe, S.; Schmuck, C.; Voskuhl, J. A Dual PH-Responsive Supramolecular Gelator with Aggregation-Induced Emission Properties. *Soft Matter* **2018**, *14* (30), 6166–6170. https://doi.org/10.1039/c8sm01190g.

(17) Adams, D. J.; Butler, M. F.; Frith, W. J.; Kirkland, M.; Mullen, L.; Sanderson, P. A New Method for Maintaining Homogeneity during Liquid-Hydrogel Transitions Using Low Molecular Weight Hydrogelators. *Soft Matter* **2009**, *5* (9), 1856–1862. https://doi.org/10.1039/b901556f.

(18) Verdejo, B.; Rodríguez-Llansola, F.; Escuder, B.; Miravet, J. F.; Ballester, P. Sodium and PH Responsive Hydrogel Formation by the Supramolecular System Calix[4]Pyrrole Derivative/Tetramethylammonium Cation. *Chem. Commun.* **2011**, *47* (7), 2017–2019. https://doi.org/10.1039/c0cc04051g.

(19) Angulo-Pachón, C. A.; Miravet, J. F. Sucrose-Fueled, Energy Dissipative, Transient Formation of Molecular Hydrogels Mediated by Yeast Activity. *Chem. Commun.* **2016**, *52* (31), 5398–5401. https://doi.org/10.1039/c6cc01183g.

(20) Wang, X.; Spencer, H. G. Calcium Alginate Gels: Formation and Stability in the Presence of an Inert Electrolyte. *Polymer (Guildf).* **1998**, *39* (13), 2759–2764. https://doi.org/10.1016/S0032-3861(97)00597-1.

(21) Suzuki, M.; Sato, T.; Kurose, A.; Shirai, H.; Hanabusa, K. New Low-Molecular Weight Gelators Based on L-Valine and L-Isoleucine with Various Terminal Groups. *Tetrahedron Lett.* **2005**, *46* (16), 2741–2745. https://doi.org/10.1016/j.tetlet.2005.02.144.

(22) Fu, X.; Wang, N.; Zhang, S.; Wang, H.; Yang, Y. Formation Mechanism of Supramolecular Hydrogels in the Presence of L-Phenylalanine Derivative as a Hydrogelator. *J. Colloid Interface Sci.* **2007**, *315* (1), 376–381. https://doi.org/10.1016/j.jcis.2007.06.013.

(23) Suzuki, M.; Yumoto, M.; Shirai, H.; Hanabusa, K. Supramolecular Gels Formed by Amphiphilic Low-Molecular-Weight Gelators of Nα-Nεdiacyl-L-Lysine Derivatives. *Chem. - A Eur. J.* **2008**, *14* (7), 2133–2144. https://doi.org/10.1002/chem.200701111.

(24) Bernet, A.; Behr, M.; Schmidt, H. W. Supramolecular Nanotube-Based Fiber Mats by

Self-Assembly of a Tailored Amphiphilic Low Molecular Weight Hydrogelator. *Soft Matter* **2011**, *7* (3), 1058–1065. https://doi.org/10.1039/c0sm00456a.

(25) Wu, J.; Lu, J.; Hu, J.; Gao, Y.; Ma, Q.; Ju, Y. Self-Assembly of Sodium Glycyrrhetinate into a Hydrogel: Characterisation and Properties. *RSC Adv.* **2013**, *3* (47), 24906–24909. https://doi.org/10.1039/c3ra43306d.

(26) Wang, D.; Hao, J. Multiple-Stimulus-Responsive Hydrogels of Cationic Surfactants and Azoic Salt Mixtures. *Colloid Polym. Sci.* **2013**, *291* (12), 2935–2946. https://doi.org/10.1007/s00396-013-3036-4.

(27) Velema, W. A.; Stuart, M. C. A.; Szymanski, W.; Feringa, B. L. Light-Triggered Self-Assembly of a Dichromonyl Compound in Water. *Chem. Commun.* **2013**, *49* (44), 5001–5003. https://doi.org/10.1039/c3cc41018h.

(28) Sun, X.; Xin, X.; Tang, N.; Guo, L.; Wang, L.; Xu, G. Manipulation of the Gel Behavior of Biological Surfactant Sodium Deoxycholate by Amino Acids. *J. Phys. Chem. B* **2014**, *118* (3), 824–832. https://doi.org/10.1021/JP409626S/SUPPL_FILE/JP409626S_SI_001.PDF.

(29) Draper, E. R.; Su, H.; Brasnett, C.; Poole, R. J.; Rogers, S.; Cui, H.; Seddon, A.; Adams, D. J. Opening a Can of Worm(-like Micelle)s: The Effect of Temperature of Solutions of Functionalized Dipeptides. *Angew. Chemie - Int. Ed.* **2017**, *56* (35), 10467–10470. https://doi.org/10.1002/anie.201705604.

(30) Roy, R.; Majumder, J.; Datta, H. K.; Parveen, R.; Dastidar, P. Supramolecular Hydrogels Developed from Mafenide and Indomethacin as a Plausible Multidrug Self-Delivery System as Antibacterial and Anti-Inflammatory Topical Gels. *ACS Appl. Bio Mater.* **2022**, *5* (2), 610–621. https://doi.org/10.1021/acsabm.1c01089.

(31) Pal, A.; Basit, H.; Sen, S.; Aswal, V. K.; Bhattacharya, S. Structure and Properties of Two Component Hydrogels Comprising Lithocholic Acid and Organic Amines. *J. Mater. Chem.* **2009**, *19* (25), 4325–4334. https://doi.org/10.1039/b903407b.

(32) Mukai, M.; Kogiso, M.; Aoyagi, M.; Asakawa, M.; Shimizu, T.; Minamikawa, H. Supramolecular Nanofiber Formation from Commercially Available Arginine and a Bola-Type Diacetylenic Diacid via Hydrogelation. *Polym. J.* **2012**, *44* (6), 646–650. https://doi.org/10.1038/pj.2012.46.

(33) Kar, T.; Mandal, S. K.; Das, P. K. Influence of Pristine SWNTs in Supramolecular Hydrogelation: Scaffold for Superior Peroxidase Activity of Cytochrome C. *Chem. Commun.* **2012**, *48* (67), 8389–8391. https://doi.org/10.1039/c2cc33593j.

(34) Weingarten, A. S.; Kazantsev, R. V.; Palmer, L. C.; Fairfield, D. J.; Koltonow, A. R.; Stupp, S. I. Supramolecular Packing Controls H2 Photocatalysis in Chromophore Amphiphile Hydrogels. *J. Am. Chem. Soc.* **2015**, *137* (48), 15241–15246. https://doi.org/10.1021/jacs.5b10027.

(35) Nandi, N.; Basak, S.; Kirkham, S.; Hamley, I. W.; Banerjee, A. Two-Component Fluorescent-Semiconducting Hydrogel from Naphthalene Diimide-Appended Peptide with Long-Chain Amines: Variation in Thermal and Mechanical Strengths of Gels. *Langmuir* **2016**, *32* (49), 13226–13233. https://doi.org/10.1021/acs.langmuir.6b02727.

(36) Bieser, A. M.; Tiller, J. C. Structure and Properties of an Exceptional Low Molecular Weight Hydrogelator. *J. Phys. Chem. B* **2007**, *111* (46), 13180–13187. https://doi.org/10.1021/jp074953w.

(37) Gräbner, D.; Zhai, L.; Talmon, Y.; Schmidt, J.; Freiberger, N.; Glatter, O.; Herzog, B.; Hoffmann, H. Phase Behavior of Aqueous Mixtures of 2-Phenylbenzimidazole-5-Sulfonic Acid and Cetyltrimethylammonium Bromide: Hydrogels, Vesicles, Tubules, and Ribbons. *J. Phys. Chem. B* **2008**, *112* (10), 2901–2908. https://doi.org/10.1021/jp0749423.

(38) Raghavan, S. R.; Cipriano, B. H. Gel Formation: Phase Diagrams Using Tabletop Rheology and Calorimetry. In *Molecular Gels: Materials with Self-Assembled Fibrillar Networks*; Weiss, R. G., Terech, P., Eds.; Springer Netherlands: Dordrecht, 2006; pp

241–252. https://doi.org/10.1007/1-4020-3689-2_9.

(39) Fuhrhop, J. H.; Helfrich, W. Fluid and Solid Fibers Made of Lipid Molecular Bilayers. *Chem. Rev.* **1993**, *93* (4), 1565–1582. https://doi.org/10.1021/cr00020a008.

(40) Fuhrhop, J. H.; Schnieder, P.; Boekema, E.; Helfrich, W. Lipid Bilayer Fibers from Diastereomeric and Enantiomeric N-Octylaldonamides. *J. Am. Chem. Soc.* **1988**, *110* (9), 2861–2867. https://doi.org/10.1021/ja00217a028.

(41) Ananthapadmanabhan, K. P.; Goddard, E. D.; Turro, N. J.; Kuo, P. L. Fluorescence Probes for Critical Micelle Concentration. *Langmuir* **1985**, *1* (3), 352–355. https://doi.org/10.1021/la00063a015.

(42) Escuder, B.; LLusar, M.; Miravet, J. F. Insight on the NMR Study of Supramolecular Gels and Its Application to Monitor Molecular Recognition on Self-Assembled Fibers. *J. Org. Chem.* **2006**, *71* (20), 7747–7752. https://doi.org/10.1021/jo0612731.

(43) Saito, M.; Moroi, Y.; Matuura, R. Dissolution and Micellization of Sodium N-Alkylsulfonates in Water. *J. Colloid Interface Sci.* **1982**, *88* (2), 578–583. https://doi.org/10.1016/0021-9797(82)90286-7.

(44) Miravet, J. F.; Escuder, B.; Segarra-Maset, M. D.; Tena-Solsona, M.; Hamley, I. W.; Dehsorkhi, A.; Castelletto, V. Self-Assembly of a Peptide Amphiphile: Transition from Nanotape Fibrils to Micelles. *Soft Matter* **2013**, *9* (13), 3558–3564. https://doi.org/10.1039/c3sm27899a.

(45) Sayar, M.; Stupp, S. I. Assembly of One-Dimensional Supramolecular Objects: From Monomers to Networks. *Phys. Rev. E - Stat. Nonlinear, Soft Matter Phys.* **2005**, *72* (1), 011803. https://doi.org/10.1103/PhysRevE.72.011803.

(46) Dreiss, C. A. Hydrogel Design Strategies for Drug Delivery. *Current Opinion in Colloid and Interface Science*. Elsevier August 1, 2020, pp 1–17. https://doi.org/10.1016/j.cocis.2020.02.001.

(47) Dorishetty, P.; Dutta, N. K.; Choudhury, N. R. Bioprintable Tough Hydrogels for

Tissue Engineering Applications. *Advances in Colloid and Interface Science*. Elsevier July 1, 2020, p 102163. https://doi.org/10.1016/j.cis.2020.102163.

(48) Chivers, P. R. A.; Smith, D. K. Shaping and Structuring Supramolecular Gels. *Nature Reviews Materials*. Nature Publishing Group May 23, 2019, pp 463–478. https://doi.org/10.1038/s41578-019-0111-6.

(49) Janni, D. S.; Rajput, G.; Pandya, N.; Subramanyam, G.; Varade, D. Interfacial Properties of Novel Surfactants Based on Maleic and Succinic Acid for Potential Application in Personal Care. *J. Mol. Liq.* **2021**, *342*, 117484. https://doi.org/10.1016/j.molliq.2021.117484.

SUPPORTING INFORMATION

Alkaline cations dramatically control molecular hydrogelation by an amino acid-derived anionic amphiphile

*César A. Angulo-Pachón, Victor Pozo, and Juan F. Miravet**

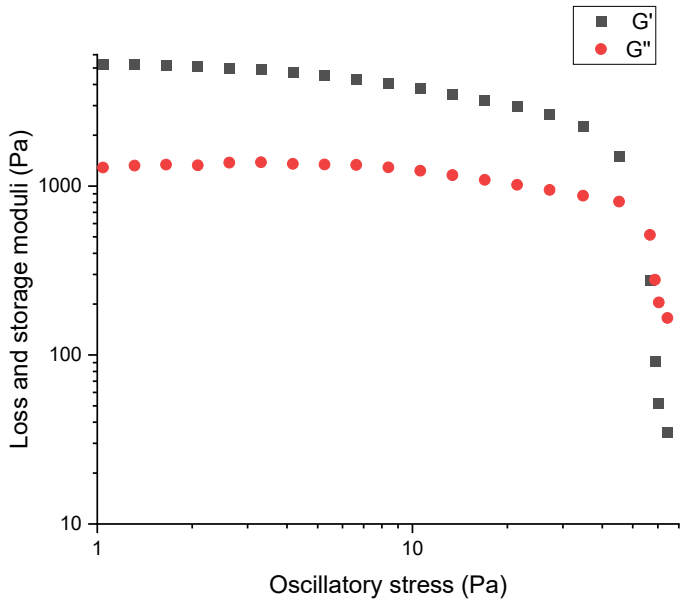

Figure S1. Rheological study of the hidrogel formed by **DodValSuc** (26 mM) in the presence of 1M Na^+.

NMR SPECTRA

Figure S2. ^{1}H-NMR spectrum of ButBoc in $CDCl_3$

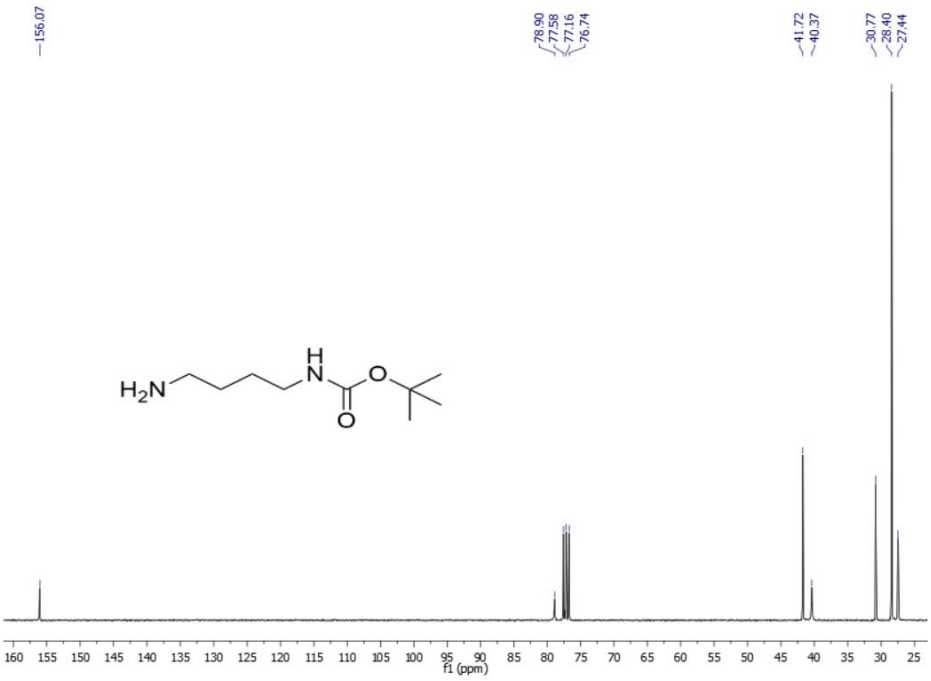

Figure S3. ^{13}C-NMR spectrum of ButBoc in $CDCl_3$

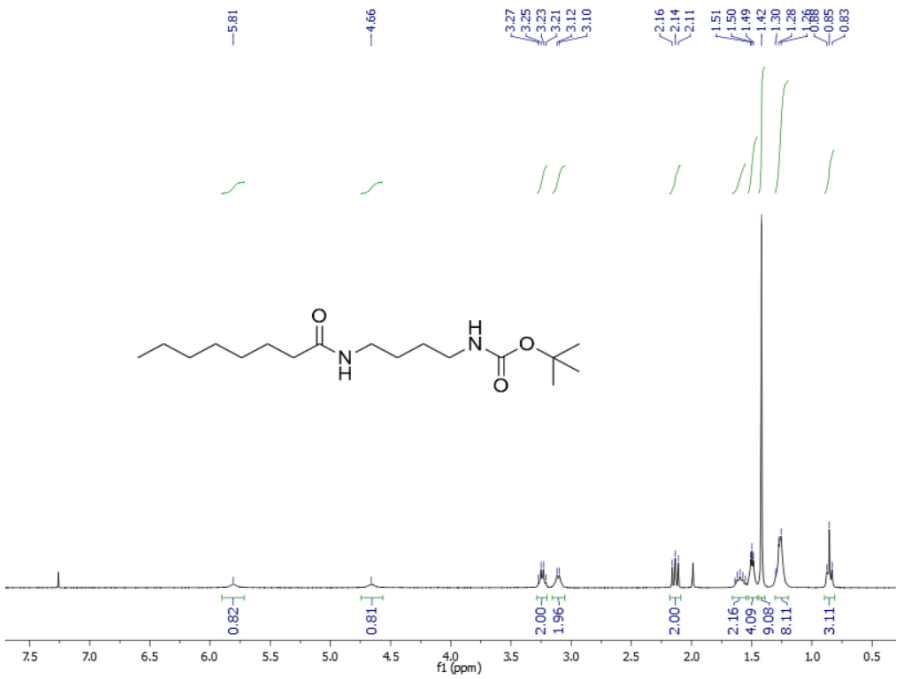

Figure S4. ^{1}H-NMR spectrum of **OctButBoc** in $CDCl_3$

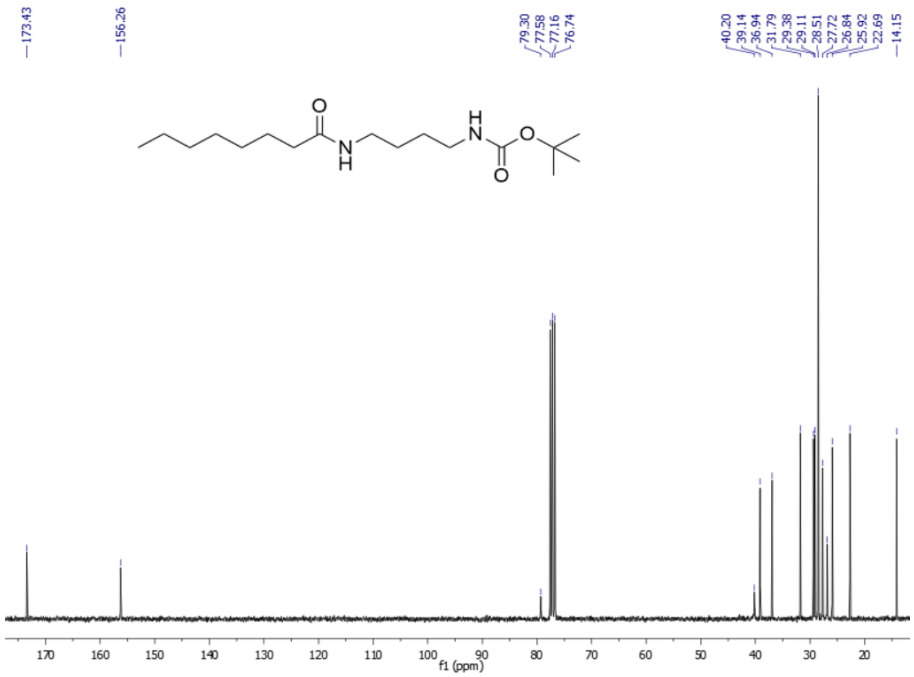

Figure S5. ^{13}C-NMR spectrum of **OctButBoc** in $CDCl_3$

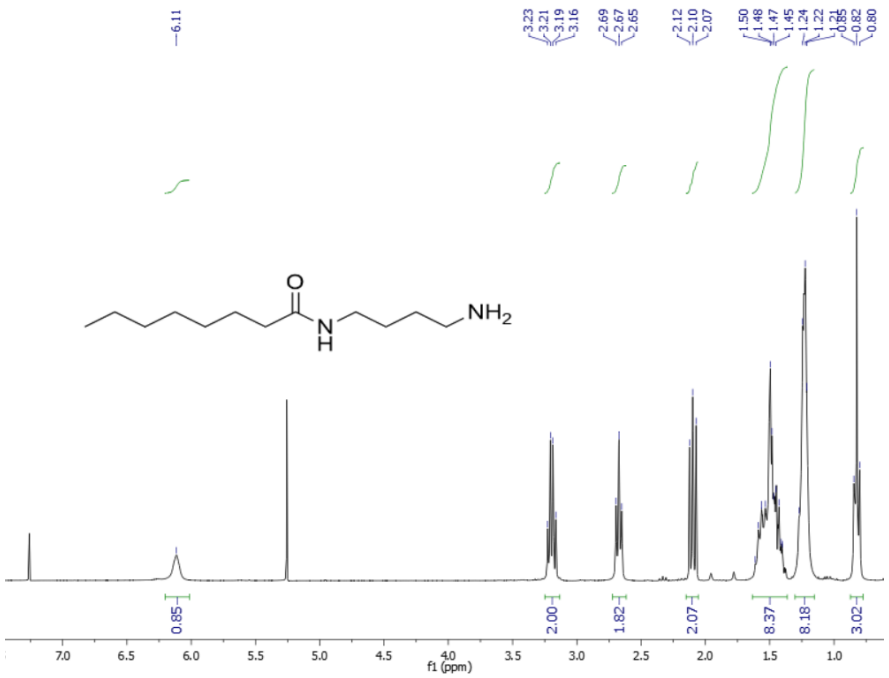

Figure S6. ^{1}H-NMR spectrum of **OctBut** in $CDCl_3$

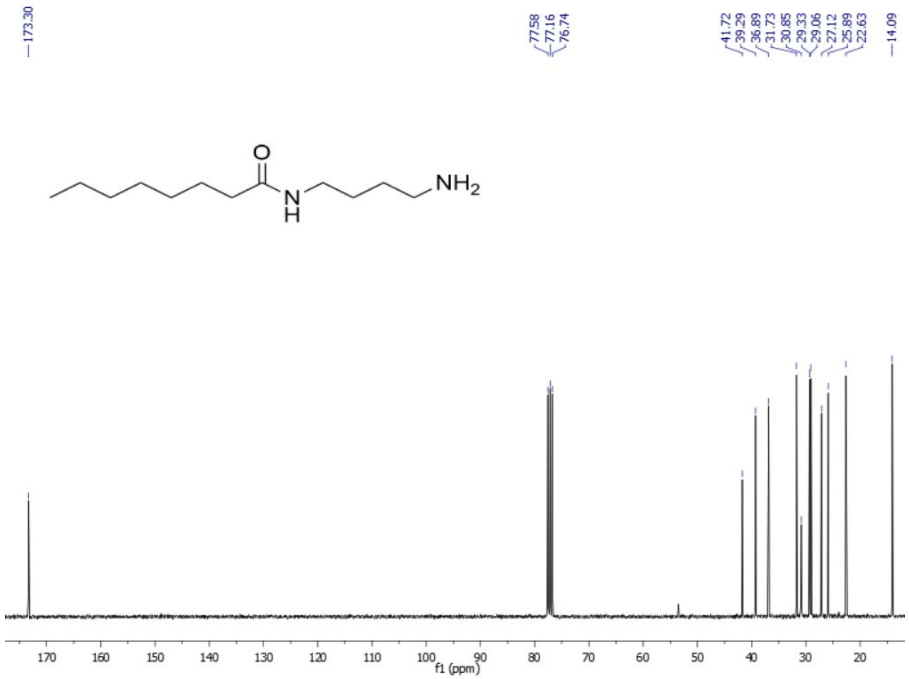

Figure S7. ^{13}C-NMR spectrum of **OctBut** in $CDCl_3$

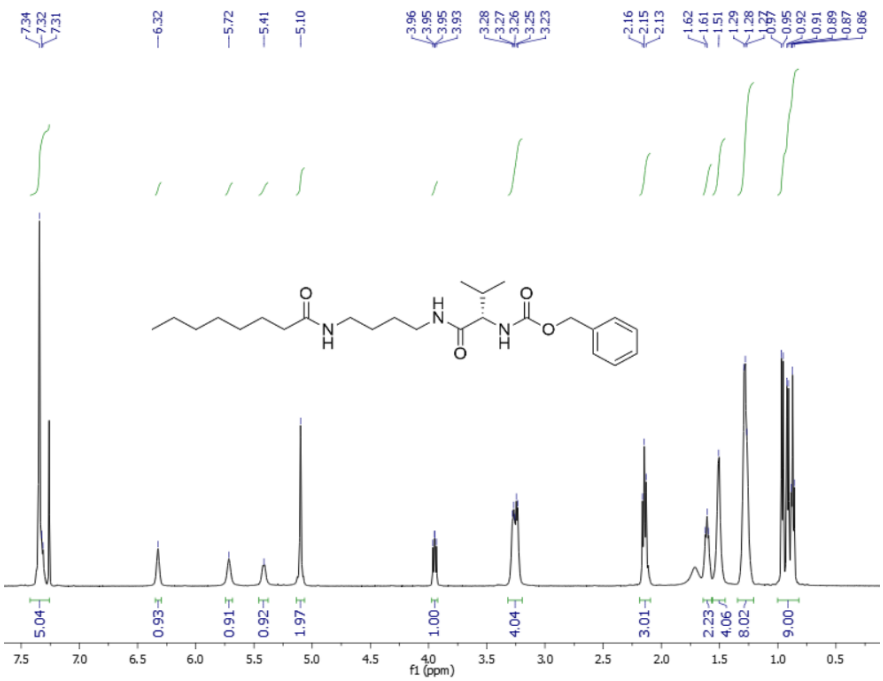

Figure S8. ^{1}H-NMR spectrum of **OctButValZ** in $CDCl_3$

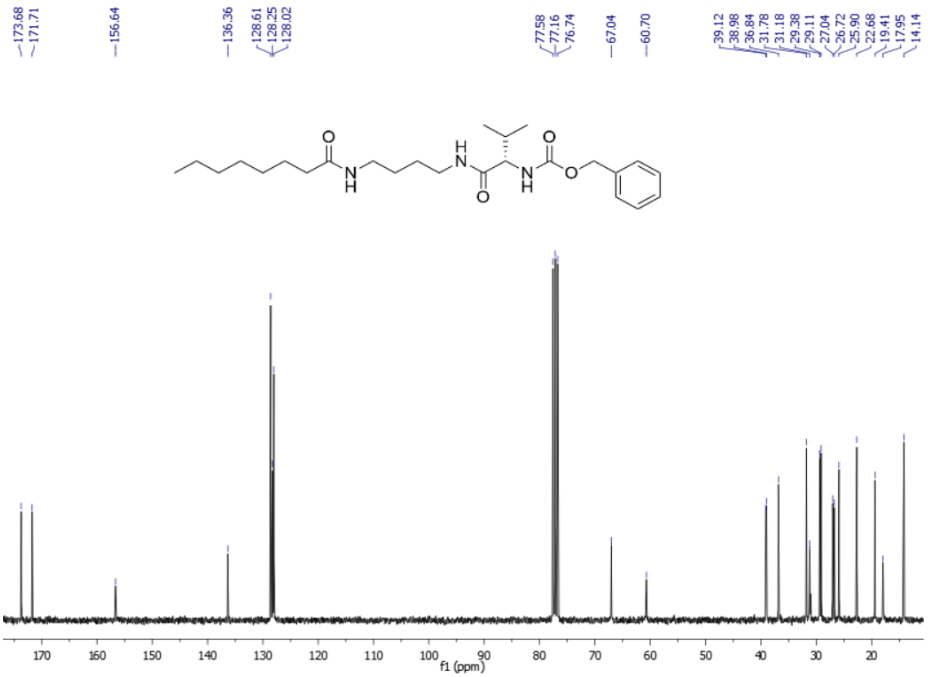

Figure S9. ^{13}C-NMR spectrum of **OctButValZ** in $CDCl_3$

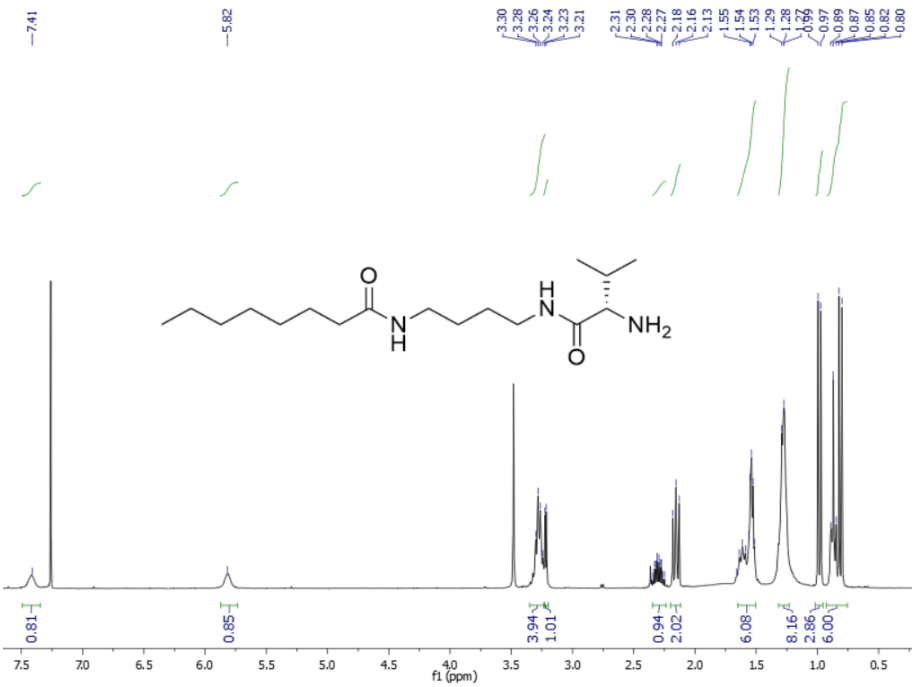

Figure S10. ^{1}H-NMR spectrum of **OctButVal** in $CDCl_3$

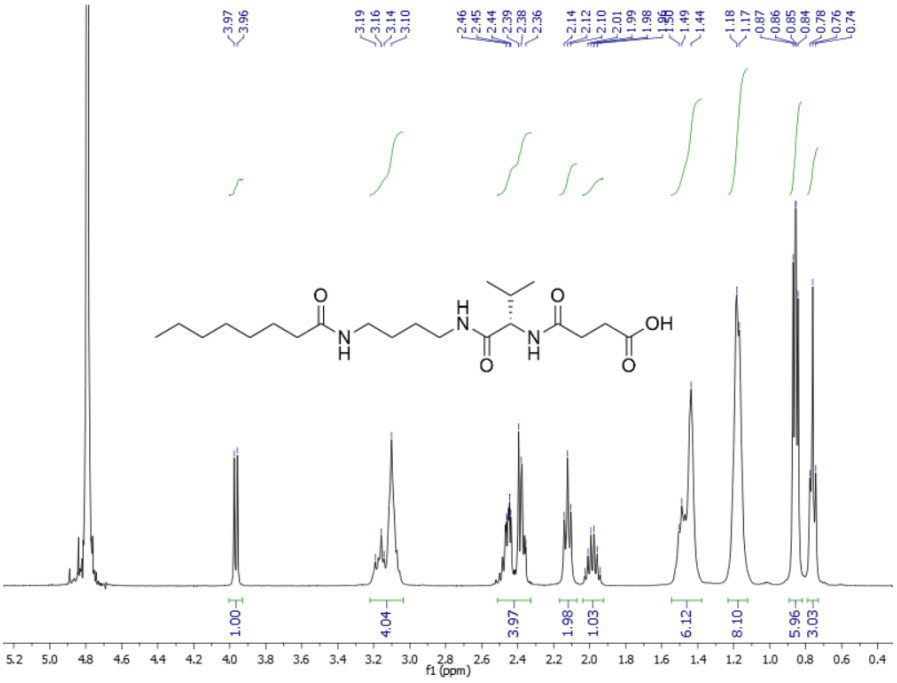

Figure S11. ^{1}H-NMR spectrum of **OctButValSuc** in D_2O

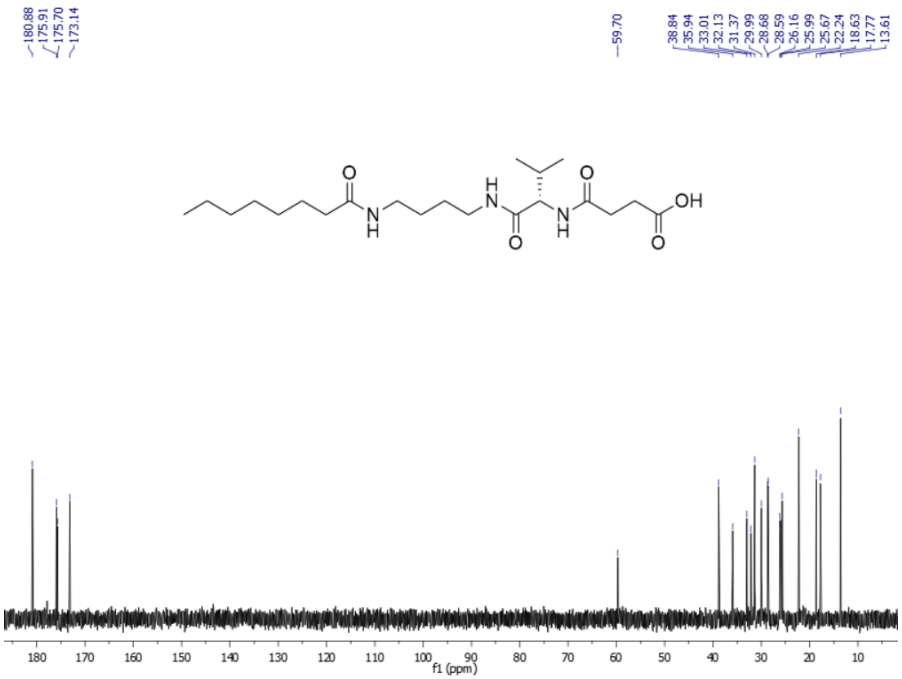

Figure S12. ^{13}C-NMR spectrum of **OctButValSuc** in D_2O

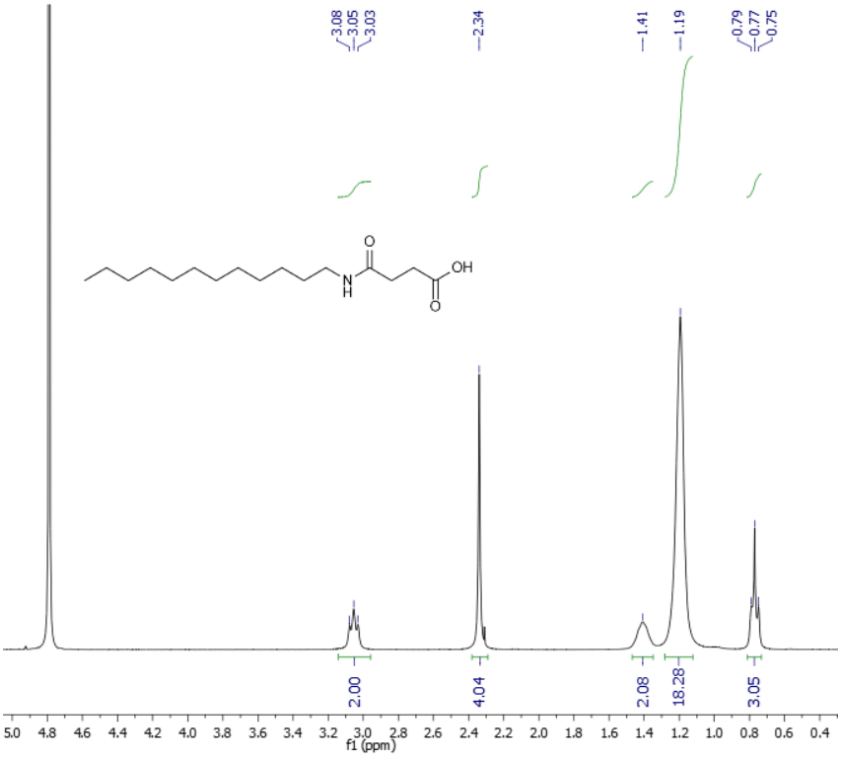

Figure S13. ^{1}H-NMR spectrum of **DodSuc** in D_2O

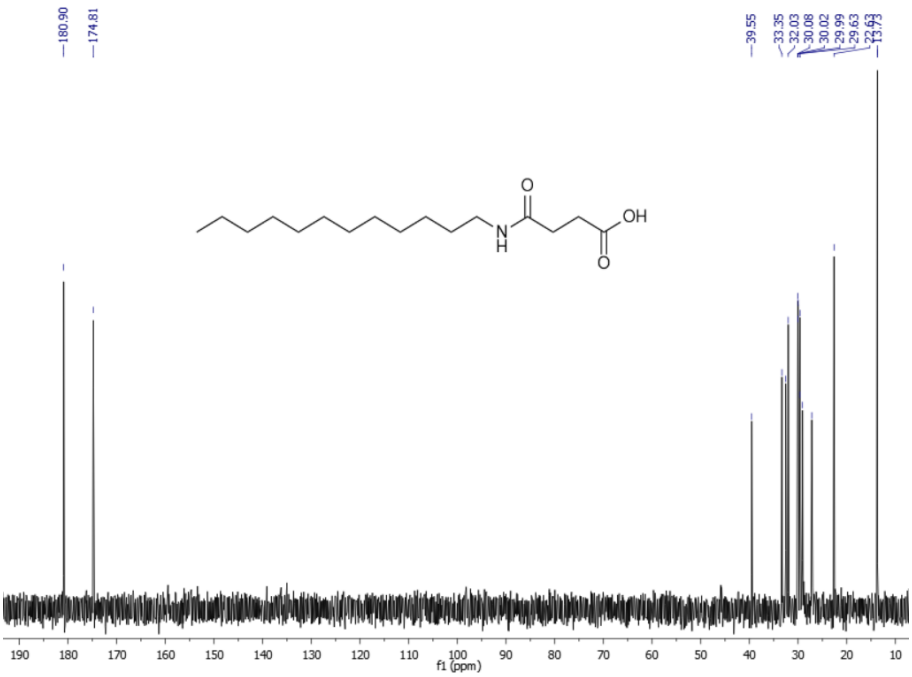

Figure S13. ^{13}C-NMR spectrum of **DodSuc** in D_2O

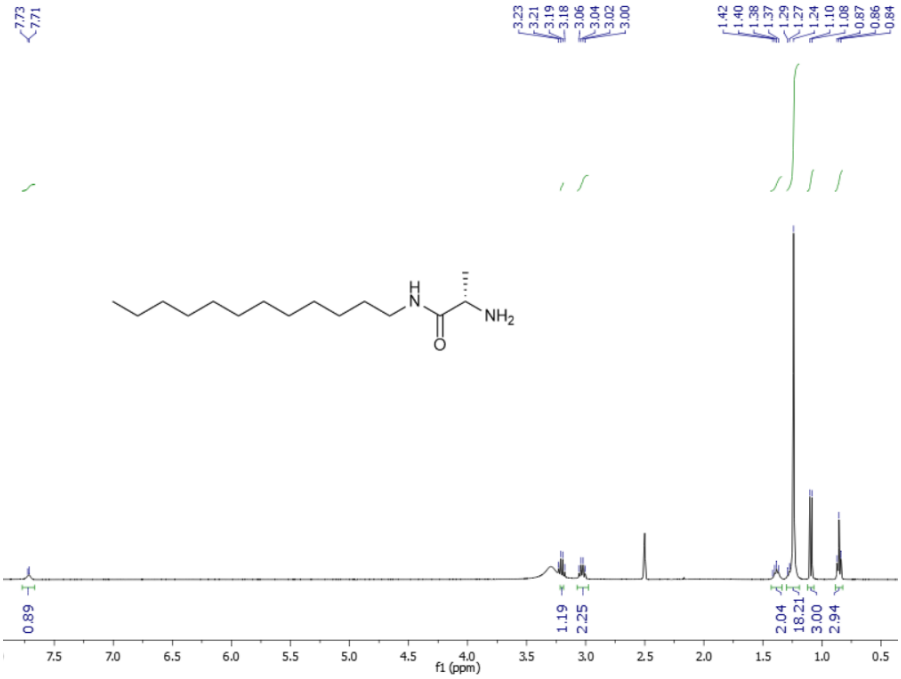

Figure S14. ^{1}H-NMR spectrum of **DodVal** in DMSO-d_6